

Study on Flame Stabilization in a SCRAMJET Engine using OH-PLIF Imaging

Pinto Rocky Simon^{a,*}, Sree Renganathan T^b, S. M. D. Hamid Ansari^c, T. M. Muruganandam^d

^a Senior Research Fellow, National Centre for Combustion Research and Development (NCCRD), Indian Institute of Technology Madras, Chennai, India, aerok12939@gmail.com

^b Senior Project Officer, NCCRD, Indian Institute of Technology Madras, Chennai, India, thanusr4@gmail.com

^c Project Associate, NCCRD, Indian Institute of Technology Madras, Chennai, India, hameedansari789@gmail.com

^d Professor, NCCRD, Dept of Aerospace Engineering, Indian Institute of Technology Madras, Chennai, India, murgi@smail.iitm.ac.in.

Abstract

The transient nature of flame stabilization in a strut-stabilized supersonic combustor is presented in this paper. The experiments are performed using an H₂-O₂ combustion-based vitiator to vitiate the air to stagnation properties of 1405 K and 8.65 bar. The H₂ fuel is injected into an M 2.5 flow through five 2.5 mm holes on either side of a strut. High-speed flame imaging is used to detect the flame transitions between two modes. A high-speed shadowgraph is used to study the shock system generated by the strut. Simultaneous OH* chemiluminescence and 10 Hz OH PLIF (Planar Laser-Induced Fluorescence) imaging are used to study the region of heat release and post-flame structure at the fuel jet and in the wake of the strut. Two combustion modes (CM) were observed at the strut; namely, strut wake stabilized flame (CM1) and fuel jet stabilized flame stabilization modes (CM2).

1. Introduction

Scramjets are of growing interest for their application in defense and space explorations [1]–[3]. Research on supersonic combustors is of significant importance for developing scramjets [4]–[6]. To have a sustainable stable thrust, the flame should stabilize within the combustor and have minimum ignition delay [7]. Different types of flame holders used to stabilize the flame are ramps [8]–[11], cavities [12]–[14], and struts [15]. Strut provides uniform penetration at the expense of the total pressure losses. The current study uses the strut to stabilize the supersonic combustor flame [16]–[20]. The use of hydrogen as a suitable fuel for scramjet is discussed by [21]–[23]. It was reported that hydrogen fuel provides higher heat release, lower ignition delay, and better stabilization when compared to other fuels. Hence, hydrogen is used for flame stabilization studies in a supersonic combustor.

For developing a supersonic combustor, research on ignition and flame stabilization for different flame holders, fuels, and different inlet conditions is essential. Yu *et al.* [44] experimentally investigated the effect of flame-holding cavities on the performance of the supersonic combustor. The effect of different configurations of open cavities on combustion performance was reported. Liu *et al.* [24] studied the ignition and flame stabilization in a cavity stabilized ethylene fueled scramjet engine. It was reported that after ignition, the hot products and high temperature trapped in the cavity enable the flame to be stabilized in the cavity. Tian *et al.* [25] experimentally studied the flame growth and stabilization in kerosene-fueled cavity stabilized supersonic combustor. Ruan *et al.* [26] studied the combustion mode in cavity stabilized supersonic combustion. It was reported that high static temperature helps in flame stabilization inside the cavity. Shi *et al.* [27] experimentally studied the flame stabilization characteristics for an ethylene-fueled cavity stabilized scramjet engine using a hydrogen pilot. It was reported that pilot hydrogen enabled the ignition and stabilization at a very low equivalence ratio. Kato *et al.* [28] studied the flame dynamics occurring in a supersonic combustor under various back pressures. Higher back pressure was reported to enhance the transition from scram to ram mode in a dual-mode engine. Thakor *et al.* [29] experimentally and numerically studied the flame stabilization in a strut-stabilized hydrogen-fueled supersonic combustor. Wu *et al.* [30] reported multiple flame stabilization modes for a strut-stabilized hydrogen-fueled supersonic combustor.

The flame stabilization in the supersonic combustor is highly transient in nature [31]–[37]. The flame stabilization modes in a supersonic combustor depend on the local static temperature, injection pressure, and injection mechanism [38]. Wang *et al.* [36] discussed the periodical transition in a hydrogen-fueled scramjet combustor

stabilized using a cavity. It was reported that the combustion mode oscillates between two modes for fixed inlet conditions and fuel equivalence ratio. Zhao *et al.* [39] studied the combustion oscillation caused by the change in cavity parameters. Yang *et al.* [40] reported the mechanism of combustion mode transitions in hydrogen-fueled scramjet engines. Bao *et al.* [41] reported three combustion modes in a strut-stabilized supersonic combustor. Two ram modes and one scram mode were reported. Yan *et al.* [42] reported the nonlinear transition process between modes in a typical strut-based and a cavity-based supersonic combustor. Chang *et al.* [43] experimentally studied the hysteresis occurring in a strut-equipped scramjet engine. Yan *et al.* [44] studied hysteresis in a dual strut scramjet engine. Zhang *et al.* [45] and Zhang *et al.* [46] numerically studied the mode transitions in cavity-stabilized supersonic combustors. Pinto *et al.* [47] studied the occurrence of hysteresis in flame stabilization modes for varying ER. Hysteresis was observed between fuel jet stabilized mode and strut wake stabilized mode for changing equivalence ratio (ER) for lower stagnation temperatures. Hence, further study is required to investigate the effect of change in equivalence ratio on flame stabilization in a strut-stabilized supersonic combustor for higher stagnation temperatures.

Zhao *et al.* [48] studied the effects of injection parameters on flashbacks occurring in a cavity-stabilized supersonic combustor. It was reported higher injection angle, higher ER, and multiple injection points led to intense combustion and flashback. Sun *et al.* [49] studied the occurrence of flashbacks in an ethylene-fueled cavity stabilized supersonic combustor. It was reported that higher global ER at the injection point led to flashbacks near the injection point. Zhang *et al.* [50] reported flashbacks in strut-wall stabilized supersonic combustors. It was reported that the flashback occurs when the injection shock separates the boundary layer near the wall forming recirculation pockets. Zhu *et al.* [51] studied the flashback phenomenon in a staged strut scramjet engine. It was reported that the flash occurred at a higher stagnation temperature, and ER was caused by the propagation of the detonation wave. Hence, it is important to study further the flashback phenomenon caused by higher ER and injection pressure.

In the current work, the flame transitions and flashback occurring for varying equivalence ratio is studied using high-speed flame imaging. Simultaneous OH* chemiluminescence and OH PLIF is used to study the flame structure of the strut stabilized flame.

2. Experimental methods

2.1 Supersonic combustor test rig

A supersonic combustion test rig designed and operated at the National Centre for Combustion Research and Development (NCCRD), Indian Institute of Technology Madras, was used for the experimental studies. Figure 1 and Fig. 2 illustrate the experimental rig used for the current work. The supersonic combustion test rig has five parts: an H₂-O₂ vitiator, rectangular cross-section convergent-divergent nozzle, isolator, combustor, and a divergent section. Six individual H₂-O₂ burners are used to vitiate the air. Pressure-regulating valves (PRVs) and a choked orifice control the mass flow rates to the vitiator and the supersonic combustor. A special type of zirconia paint is used to reduce heat transfer losses from the vitiator [54]. Air is vitiated to stagnation conditions of $T_0 = 1405$ K, $P_0 = 8.65$ bar, and expanded to Mach number 2.5. The oxygen content of the air exiting the vitiator is maintained at a 21 % mole fraction using makeup oxygen. The supersonic combustor is manufactured based on the design by Tomioka *et al.* [55]. Hydrogen fuel is injected transversely through 5 holes of 2.5 mm diameter each, placed at the top and the bottom of the strut as shown in Fig. 1. These rows of holes were 8 mm downstream of the step in the strut.

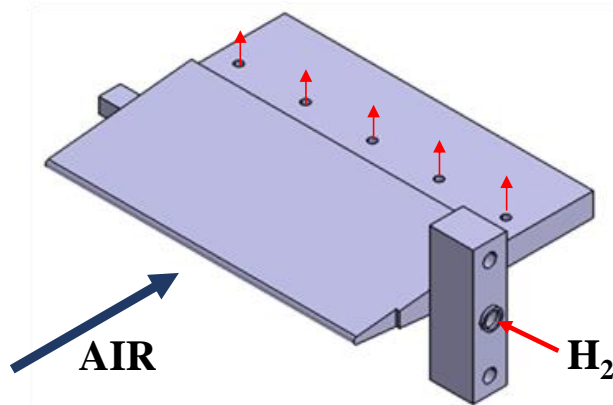


Figure 1: Strut injection mechanism

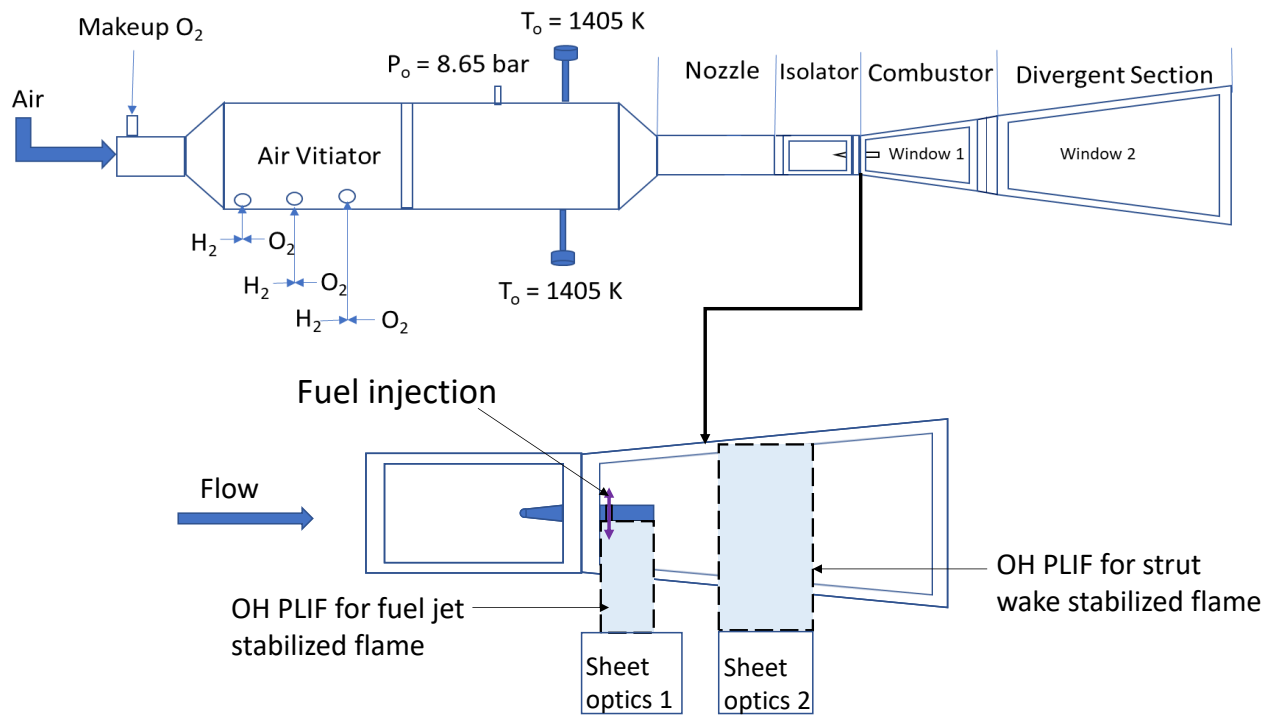


Figure 2: Supersonic combustion test rig

The test cycle of 30 seconds is shown in Fig. 3. The entire test is an autocycle controlled by a Programmable Logic Controller (PLC). The vitiator is ignited at the 7th second. Fuel in the supersonic combustor is injected at the 8th second. The scramjet engine operation is observed for 7 seconds. The equivalence ratio at the strut is varied throughout the 7 seconds of the scramjet operation. The stagnation temperature is measured at the exit of the preheater using two s-type thermocouples at 100 Hz. The stagnation temperature in Fig. 3 is maintained for the entire scramjet operation. The pressures were measured using a Wika S-20 pressure sensor at 1000 Hz. The stagnation pressure is constant throughout the scramjet operation.

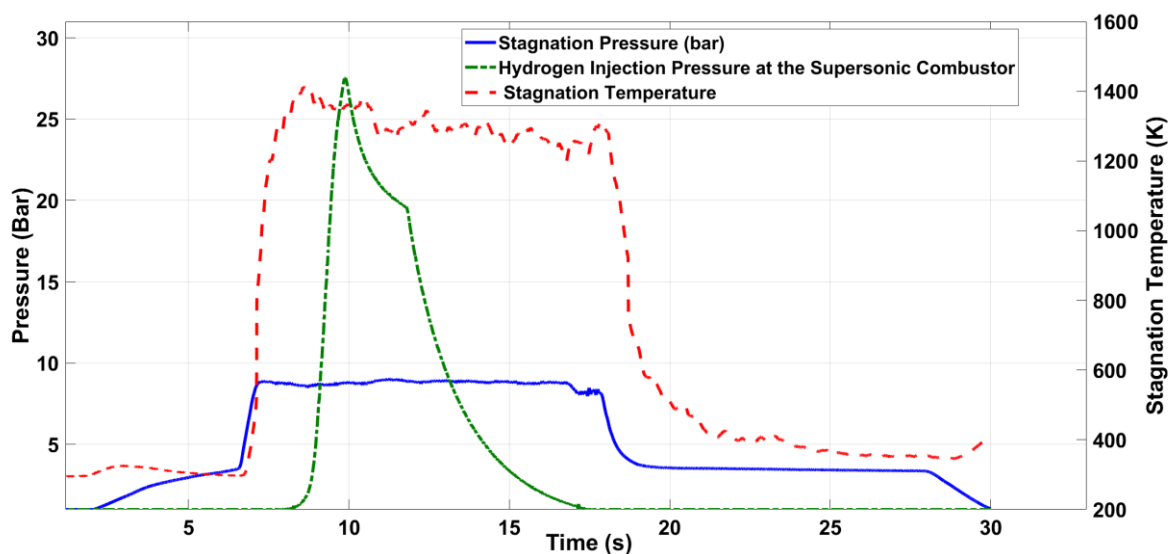


Figure 3: Supersonic combustion test cycle

2.2 Measurements and diagnostics

OH* chemiluminescence and OH PLIF were observed using quartz window one as seen in Fig. 2. Windows 1 and 2 were used to acquire high-speed flame luminosity images. FASTCAM SA 1.1 high-speed camera and a 50 mm wide-angle lens were used for recording flame images at 4000 Hz. This camera could visualize visible and near IR emissions from the flame. Thus, this will show the products of combustion. OH* chemiluminescence was captured using a PIMAX 4 intensified camera, UV lens with a focal length of 100 mm, and a filter with 310 ± 5 nm transmissivity at 10 Hz. The OH* chemiluminescence indicates the region of heat release. Simultaneous shadowgraph was captured using a halogen light source, two parabolic mirrors of the focal length of 2 m, a plane mirror, and a FASTCAM SA 1.1 high-speed camera coupled with a 100 mm lens. The OH Planar Laser-Induced Fluorescence set up for each region of interest consists of Quantel – YG980 Q-Switched Nd:YAG laser pumping the Tunable Dye Laser: Quantel TDL-90 with an output beam of 565.84 nm wavelength. This output is frequency-doubled to 282.92 nm for exciting the OH radicals in the flow. This line is chosen for its low dependence on temperature. The static pressures in the region of interest are low, reducing the collision broadening. The laser energy is of the order of 15 mJ at the exit of the laser. As seen in Fig. 2, the two regions of interest for OH PLIF are the fuel injection zone and the wake of the strut. Due to design constraints, there is no optical access at the base of the strut. For the PLIF at the strut wake (sheet optics 1), a laser sheet is formed using a cylindrical lens with a focal length of 25 mm and a spherical lens with a focal length of 500 mm. The PLIF images were captured at around 90 mm downstream of the strut base. For the PLIF at the fuel injection point (sheet optics 2), a laser sheet is formed using a cylindrical lens with a focal length of 75 mm and a spherical lens with a focal length of 500 mm. The fluorescence was captured using an intensified camera PIMAX 3, a 100 mm UV lens, and a filter with 310 ± 5 nm transmissivity at 10 Hz. All PLIF images were corrected for shot-to-shot variations. The Q-switch of the pumping laser was used to trigger the BNC 575 pulse delay generator to synchronize all equipment used in the experiment. All images were corrected for background before analysis.

3. Results and discussion

The two flame stabilization modes observed for varying ER are shown in Fig. 4. For lower ER, the flame stabilizes at the strut wake (CM1). The shock system captured at the strut is shown in Fig. 5. The step on the strut before the injection point, along with the injection shock, forms the first set of the oblique shocks seen in Fig. 5. The turning shocks generated at the base of the strut are also marked in Fig. 5. The shock system caused by the strut raises the local static temperature of the mixture above the autoignition temperature. After ignition, the recirculation zone at the wake of the strut stabilizes the flame. For higher ER, the stronger injection shock further increases the local static temperature of the mixture. The stronger injection shock reduces the local velocity near the wall of the strut. The increase in global ER and local static temperature increases the flame speed. As the flame speed is higher than the local velocity close to the strut wall, the flame flashes back to the fuel jet (CM2). The two stabilization modes observed will be discussed in the subsequent section.

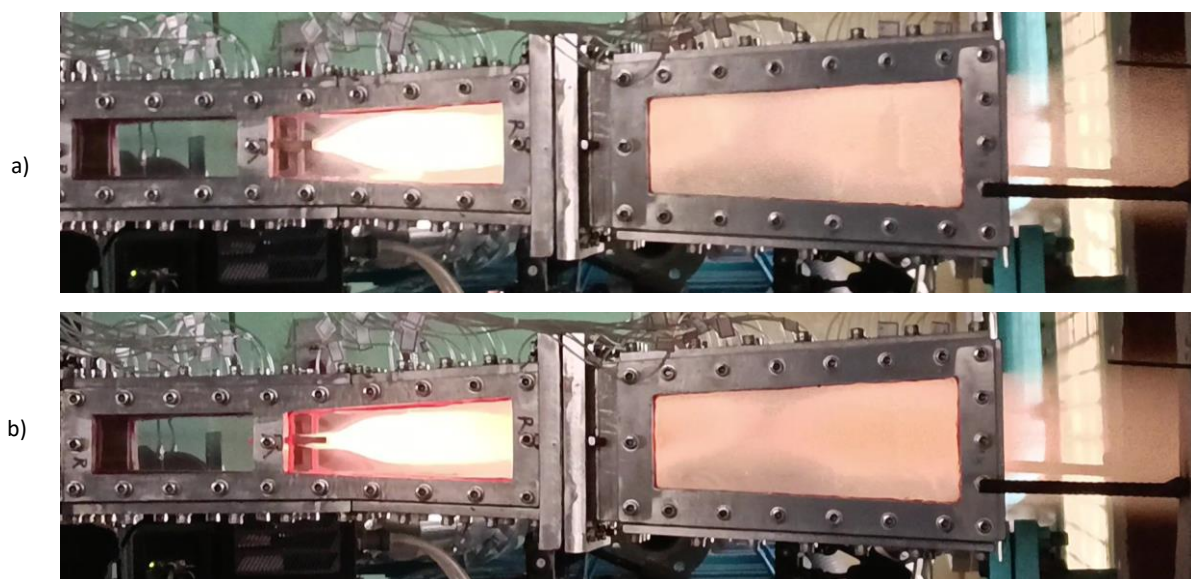


Figure 4: Flame stabilization modes: a) strut wake stabilized (CM1) and b) fuel jet stabilized (CM2)

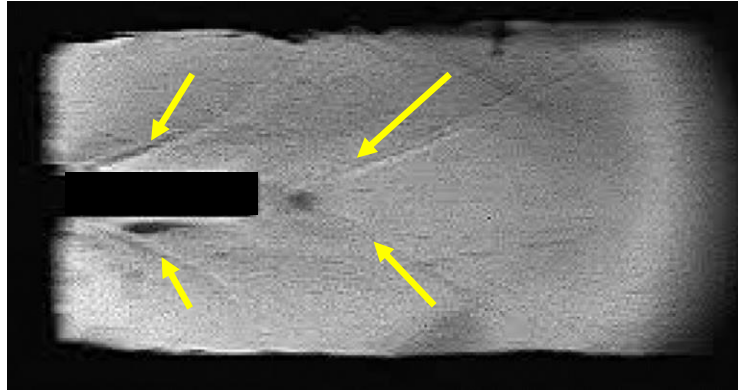


Figure 5: High-speed shadowgraph at the strut injection point

3.1 Strut wake stabilization

At lower ERs, the flame stabilizes in the wake of the strut. The flame image of the strut stabilized flame (CM1) is shown in Fig. 6. A black rectangle marks the trailing edge of the strut. The shock system generated by the strut, as shown in Fig. 5, raises the local static temperature. The shock system at the wake of the strut ignites the combustible mixture. Once the mixture is ignited, the hot products diffuse out into the free stream through the shear layer formed at the wake of the strut. Hence, the flame spreads further into the shear layer, penetrating further into the supersonic unburnt mixture. The recirculation zones at the base of the strut carry the hot products and free radicals back to the incoming unburnt mixture, stabilizing the flame.

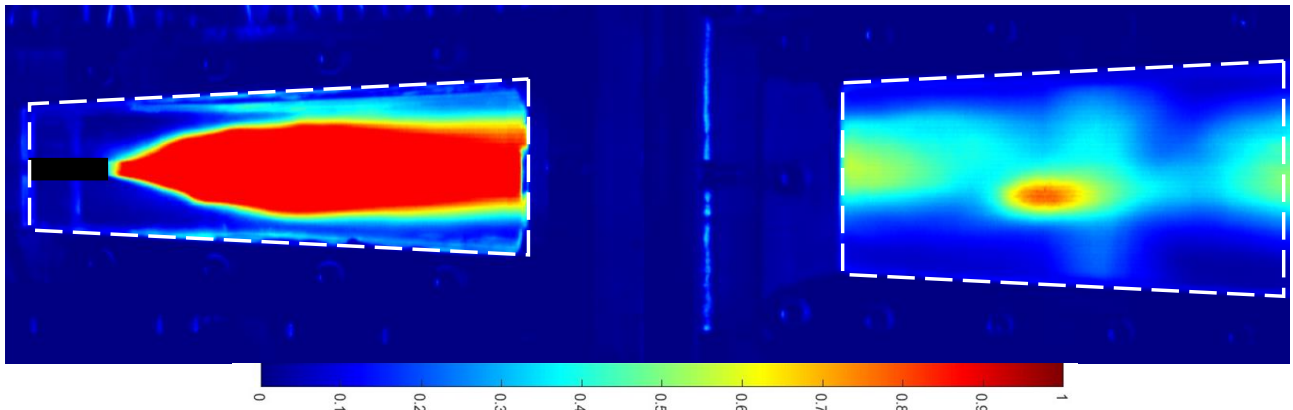


Figure 6: Flame imaging of strut stabilized flame (CM1)

Figure 7 shows the OH* chemiluminescence captured in the wake of the strut CM1. A black rectangle marks the trailing end of the strut. As seen in Fig. 7, the heat release region is mainly at the shear layer generated downstream of the strut. It is inferred that the shear layer formed by the wake of the strut is essential to stabilize the flame. The weak OH* chemiluminescence in the center line of the strut base suggests less intense combustion occurring in the region.

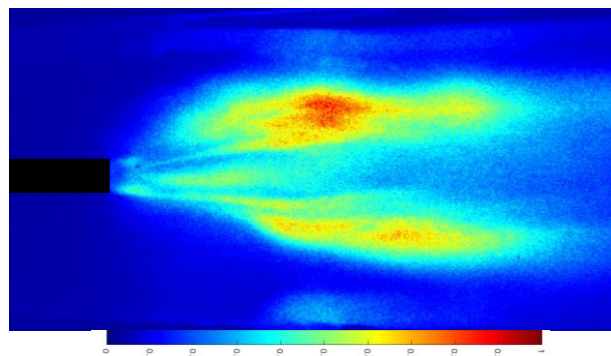


Figure 7: OH* chemiluminescence of strut stabilized flame (CM1)

Figure 8 shows the averaged OH PLIF signal captured downstream of the strut. The strut base is marked with a black rectangle. A white dashed rectangle indicates the laser sheet. The intensity in Fig. 8 is directly proportional to the concentration of OH radicals in the given plane. A strong presence of OH radicals is seen in the core of the wake of the strut. The OH radicals formed by the reaction are recirculated at the base of the strut enabling the flame to be stabilized in the wake of the strut for very low ERs.

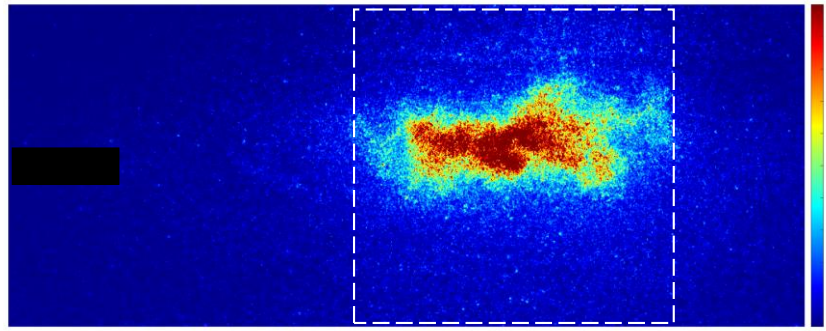


Figure 8: OH PLIF captured at the base of the strut for CM1

3.2 Fuel jet stabilization

Figure 9 shows the flame luminosity of the flame transitioning from the strut wake to the fuel jet stabilized flame (CM2). The strut trailing edge is marked using a black rectangle. At higher ER, the momentum flux of the fuel increases, creating a stronger injection shock. The stronger injection shock further reduces the local velocity near the strut wall. The local static temperature rises downstream of the injection shock, increasing the flame speed locally. The increased flame speed and reduced velocity cause a flashback, as shown in Fig. 8. The flame front moves towards the injection point and stabilizes at the fuel jet. The horseshoe vortices formed by the injection of the fuel generated downstream of the injection point cause the flame to be stabilized at the fuel jet.

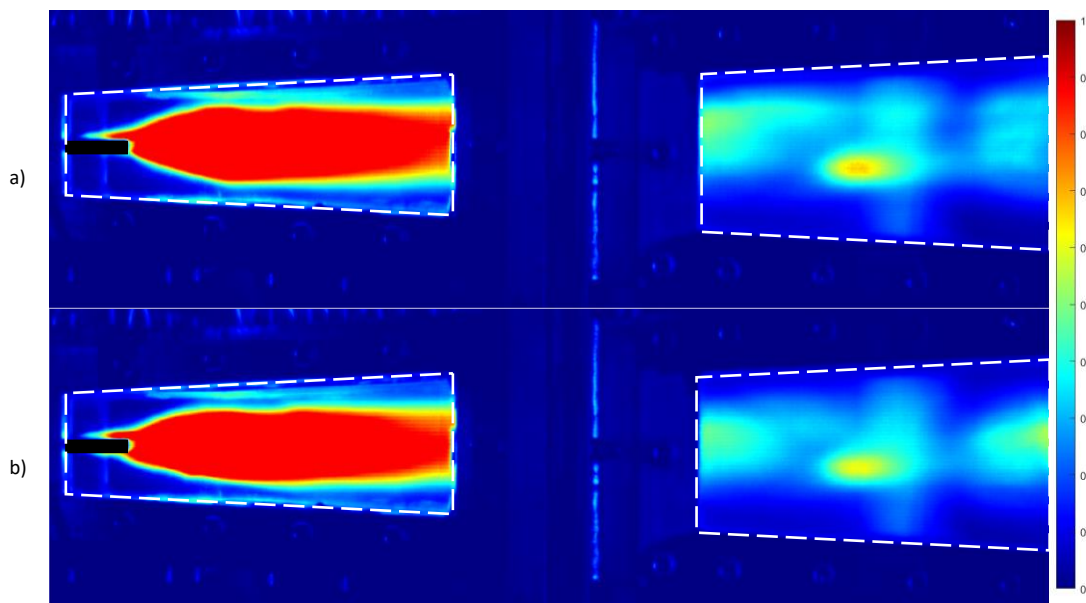


Figure 9: Flame imaging of transition of combustion mode from strut stabilized flame (CM1) to fuel jet stabilized flame (CM2)

Figure 9 shows the OH* chemiluminescence captured for the fuel jet stabilized flame for increasing ER. A black rectangle indicates the trailing edge of the strut. It can be seen in Fig 9 (a-d) that the heat release region moves upstream and stabilizes at the fuel injection point. As stated earlier, the increased ER causes an increase in the local ER and local static temperature. The enhanced flame speed causes the flame front to move upstream and stabilize at the fuel jet. A high heat release rate continues in the shear layer generated in the wake of the strut. The flame structure and the region

of heat release downstream of the strut for both modes are similar. It is suggested that the fundamental flame stabilization mechanism at the wake of the strut for both modes is similar. The flame is stabilized by the shear layer and recirculation zones formed at the strut wake.

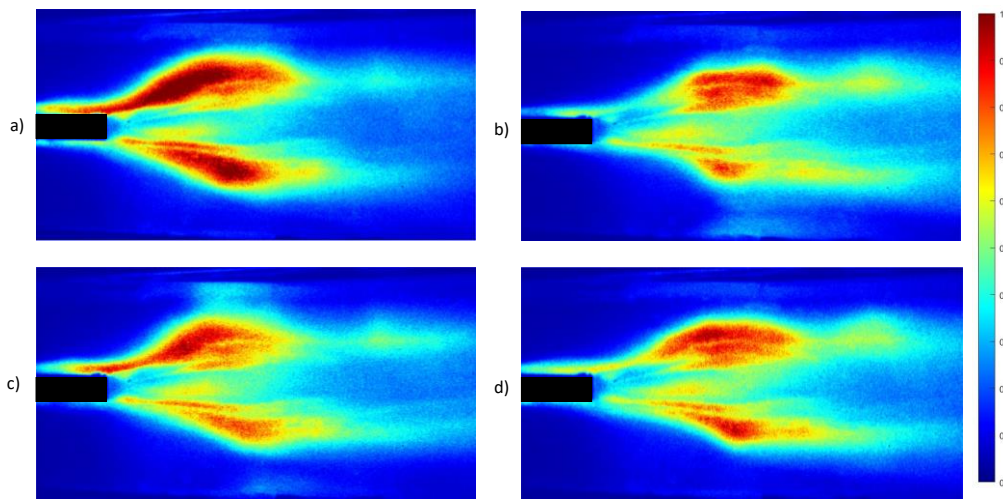


Figure 10: OH* chemiluminescence of fuel jet stabilized flame (CM2)

Figure 11 shows the OH PLIF captured at the fuel jet for the fuel jet stabilized flame stabilization mode. The strut base is marked with a black rectangle. A white dashed rectangle indicates the laser sheet. The white double arrow indicates the injection location. The intensity of Fig. 11 is directly proportional to the concentration of OH present in the region of interest. A small concentration of OH radicals is present near the injection point. It is suggested that the high temperature around the jet accelerates the rate of reaction immediately after the fuel is injected for a short distance. The concentration of OH radicals grows significantly as the combustible mixture moves downstream of the injection point. It can be seen in Fig. 11 that there is a strong presence of OH radicals downstream of the fuel injection. The recirculation of hot products through the horseshoe vortices generated by the fuel jet is critical in stabilizing the flame near the injection point. The hot OH radicals are transported to react with the incoming fuel enhancing the heat release at the injection point. Hence, the transport of OH radicals produced in the wake of the fuel jet is the primary mechanism by which flame stabilization occurs at the fuel jet.

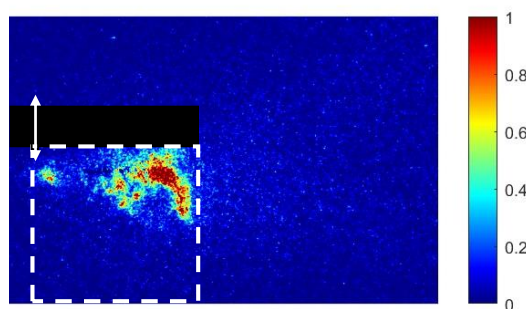


Figure 11: OH PLIF captured at the fuel jet for CM2

4. Conclusion

Experiments are performed to study the transient nature of the flame stabilization modes at the strut of the scramjet engine. High-speed imaging is used to detect the transition between flame stabilization modes. OH* chemiluminescence is captured to study the zone of heat release. 10 Hz OH PLIF is performed at the fuel injection and the strut wake to study flame stabilization modes at the strut. Two flame stabilization modes are observed at the strut. For low ER, the flame anchors at the wake of the strut. The recirculation zone at the base of the strut provides free radicals and hot products for the flame to be stabilized at the wake. The heat release region is observed in the recirculation zone and the shear layer using OH* chemiluminescence images. The presence of OH radicals in the wake indicates the availability of the hot products supplied upstream to stabilize the flame at the strut wake. Hence, the flame is stabilized at the strut wake even at very low ERs. As the ER increases, the flame flashes back and stabilizes at the fuel jet. As the ER increases, the strength of the injection shock increases, thereby decreasing the local velocity and

increasing the static temperature, which in turn increases the flame speed of the mixture. Thus, the flame flashes back to the fuel jet. The flame is stabilized at the jet wake by the free radicals, and hot products are supplied to it by the horseshoe vortices produced by the jet. The presence of OH radicals downstream of the injection point is captured using OH PLIF. The horseshoe vortices formed near the injection point transport the OH radicals to the fuel jet. This provides hot products which are necessary for the sustenance of flame at the fuel jet. The flame structure of each combustion mode and its transitions are summarized in this paper.

References

- [1] R. K. Seleznev, "History of scramjet propulsion development," *Journal of Physics: Conference Series*, vol. 1009, no. 1, 2018, doi: 10.1088/1742-6596/1009/1/012028.
- [2] E. T. Curran, "Scramjet engines: The first forty years," *Journal of Propulsion and Power*, vol. 17, no. 6, pp. 1138–1148, 2001, doi: 10.2514/2.5875.
- [3] R. K. Seleznev, S. T. Surzhikov, and J. S. Shang, "A review of the scramjet experimental data base," *Progress in Aerospace Sciences*, vol. 106, no. August 2018, pp. 43–70, 2019, doi: 10.1016/j.paerosci.2019.02.001.
- [4] Z. Ren, B. Wang, G. Xiang, D. Zhao, and L. Zheng, "Supersonic spray combustion subject to scramjets: Progress and challenges," *Progress in Aerospace Sciences*, vol. 105, no. December, pp. 40–59, 2019, doi: 10.1016/j.paerosci.2018.12.002.
- [5] T. Vanyai, M. Bricalli, S. Brieschenk, and R. R. Boyce, "Scramjet performance for ideal combustion processes," *Aerospace Science and Technology*, vol. 75, pp. 215–226, 2018, doi: 10.1016/j.ast.2017.12.021.
- [6] E. Curran, "Fluid Phenomena in Scramjet Combustion Systems," *Annual Review of Fluid Mechanics*, vol. 28, no. 1, pp. 323–360, Jan. 1996, doi: 10.1146/annurev.fluid.28.1.323.
- [7] T. Cain, "Review of Experiments on Ignition and Flameholding in Supersonic Flow," Dec. 2002. doi: 10.2514/6.2002-3877.
- [8] J. A. Fulton, J. R. Edwards, A. Cutler, J. McDaniel, and C. Goyne, "Turbulence/chemistry interactions in a ramp-stabilized supersonic hydrogen–air diffusion flame," *Combustion and Flame*, vol. 174, pp. 152–165, Dec. 2016, doi: 10.1016/j.combustflame.2016.09.017.
- [9] N. Kubo, A. Murakami, K. Kudo, and S. Tomioka, "An Experimental Investigation on Combustion Characteristics of Hypermixer Injectors—Effects of the 'Swept' Applied to Hypermixer Injector Ramps," *Procedia Engineering*, vol. 99, pp. 954–960, 2015, doi: 10.1016/j.proeng.2014.12.627.
- [10] L. S. Jacobsen, S. D. Gallimore, J. A. Schetz, W. F. O. Brien, and L. P. Goss, "An Improved Aerodynamic Ramp Injector In Supersonic Flow," *39th Aerospace Sciences Meeting & Exhibit 8-10*, no. January, 2001.
- [11] R. J. Hartfield, S. D. Hollo, and J. C. McDaniel, "Experimental investigation of a supersonic swept ramp injector using laser-induced iodine fluorescence," *Journal of Propulsion and Power*, vol. 10, no. 1, pp. 129–135, Jun. 2008, doi: 10.2514/3.23721.
- [12] Z. Wang, H. Wang, and M. Sun, "Review of cavity-stabilized combustion for scramjet applications," *Proceedings of the Institution of Mechanical Engineers, Part G: Journal of Aerospace Engineering*, vol. 228, no. 14, pp. 2718–2735, 2014, doi: 10.1177/0954410014521172.
- [13] Z. Cai, T. Wang, and M. Sun, "Review of cavity ignition in supersonic flows," *Acta Astronautica*, vol. 165, no. June, pp. 268–286, 2019, doi: 10.1016/j.actaastro.2019.09.016.
- [14] A. Ben-Yakar and R. K. Hanson, "Cavity flameholders for ignition and flame stabilization in scramjets: Review and experimental study," *34th AIAA/ASME/SAE/ASEE Joint Propulsion Conference and Exhibit*, vol. 17, no. 4, 1998.
- [15] J. Chang, J. Zhang, W. Bao, and D. Yu, "Research progress on strut-equipped supersonic combustors for scramjet application," *Progress in Aerospace Sciences*, vol. 103, no. October, pp. 1–30, Nov. 2018, doi: 10.1016/j.paerosci.2018.10.002.
- [16] L. Tian, S. Zhu, Z. Qin, X. Li, and X. Xu, "Effect of second-stage configuration on combustion in a dual-struts based staged supersonic combustor," *50th AIAA/ASME/SAE/ASEE Joint Propulsion Conference 2014*, no. 37, pp. 1–10, 2014, doi: 10.2514/6.2014-3780.
- [17] Q. Yang, W. Bao, Y. Zong, J. Chang, J. Hu, and M. Wu, "Combustion characteristics of a dual-mode scramjet injecting liquid kerosene by multiple struts," *Proceedings of the Institution of Mechanical Engineers, Part G: Journal of Aerospace Engineering*, vol. 229, no. 6, pp. 983–992, 2015, doi: 10.1177/0954410014542447.
- [18] G. Masuya *et al.*, "Ignition and Combustion Performance of Scramjet Combustors with Fuel Injection Struts," *Journal of Propulsion and Power*, vol. 11, no. 2, pp. 301–307, Jun. 1995, doi: 10.2514/3.51425.
- [19] R. P. Hande and A. G. Marathe, "A computational study on supersonic combustion with struts as flame holder," *44th AIAA/ASME/SAE/ASEE Joint Propulsion Conference and Exhibit*, no. July, pp. 1–13, 2008.

- [20] W. Huang, Z. G. Wang, S. bin Luo, and J. Liu, "Parametric effects on the combustion flow field of a typical strut-based scramjet combustor," *Chinese Science Bulletin*, vol. 56, no. 35, pp. 3871–3877, 2011, doi: 10.1007/s11434-011-4823-2.
- [21] G. Choubey, Y. D. W. Huang, L. Yan, H. Babazadeh, and K. M. Pandey, "Hydrogen fuel in scramjet engines - A brief review," *International Journal of Hydrogen Energy*, vol. 45, no. 33, pp. 16799–16815, 2020, doi: 10.1016/j.ijhydene.2020.04.086.
- [22] D. Cecere, A. Ingenito, E. Giacomazzi, L. Romagnosi, and C. Bruno, "Hydrogen / air supersonic combustion for future hypersonic vehicles," *International Journal of Hydrogen Energy*, vol. 36, no. 18, pp. 11969–11984, 2011, doi: 10.1016/j.ijhydene.2011.06.051.
- [23] D. Cecere, E. Giacomazzi, and A. Ingenito, "A review on hydrogen industrial aerospace applications," *International Journal of Hydrogen Energy*, vol. 39, no. 20, pp. 10731–10747, Jul. 2014, doi: 10.1016/J.IJHYDENE.2014.04.126.
- [24] C. Liu, M. Sun, H. Wang, L. Yang, B. An, and Y. Pan, "Ignition and flame stabilization characteristics in an ethylene-fueled scramjet combustor," *Aerospace Science and Technology*, vol. 106, p. 106186, 2020, doi: 10.1016/j.ast.2020.106186.
- [25] Y. Tian, X. Zeng, S. Yang, B. Xiao, F. Zhong, and J. Le, "Experimental study on flame development and stabilization in a kerosene fueled supersonic combustor," *Aerospace Science and Technology*, vol. 84, no. October, pp. 510–519, 2019, doi: 10.1016/j.ast.2018.10.032.
- [26] J. L. Ruan, P. Domingo, and G. Ribert, "Analysis of combustion modes in a cavity based scramjet," *Combustion and Flame*, vol. 215, pp. 238–251, 2020, doi: 10.1016/j.combustflame.2020.01.034.
- [27] W. Shi, Y. Tian, W. Zhou Zhang, W. Xin Deng, F. Yu Zhong, and J. Ling Le, "Experimental investigation on flame stabilization of a kerosene-fueled scramjet combustor with pilot hydrogen," *Journal of Zhejiang University: Science A*, vol. 21, no. 8, pp. 663–672, 2020, doi: 10.1631/jzus.A1900565.
- [28] N. Kato and S. K. Im, "Flame dynamics under various backpressures in a model scramjet with and without a cavity flameholder," *Proceedings of the Combustion Institute*, vol. 000, pp. 1–8, 2020, doi: 10.1016/j.proci.2020.07.110.
- [29] N. Thakor, C. Miranda, and S. Chaudhuri, "Flame stabilization in high enthalpy supersonic flows: Experiments and simulations," *AIAA Scitech 2020 Forum*, vol. 1 PartF, no. January, pp. 1–10, 2020, doi: 10.2514/6.2020-1841.
- [30] K. Wu, P. Zhang, W. Yao, and X. Fan, "Computational realization of multiple flame stabilization modes in DLR strut-injection hydrogen supersonic combustor," *Proceedings of the Combustion Institute*, vol. 37, no. 3, pp. 3685–3692, 2019, doi: 10.1016/j.proci.2018.07.097.
- [31] R. Masumoto, S. Tomioka, K. Kudo, A. Murakami, K. Kato, and H. Yamasaki, "Experimental study on combustion modes in a supersonic combustor," *Journal of Propulsion and Power*, vol. 27, no. 2, pp. 346–355, 2011, doi: 10.2514/1.B34020.
- [32] H. Wang, Z. Wang, M. Sun, and H. Wu, "Combustion modes of hydrogen jet combustion in a cavity-based supersonic combustor," *International Journal of Hydrogen Energy*, vol. 38, no. 27, pp. 12078–12089, Sep. 2013, doi: 10.1016/j.ijhydene.2013.06.132.
- [33] Y. Tian *et al.*, "Investigation of combustion and flame stabilization modes in a hydrogen fueled scramjet combustor," *International Journal of Hydrogen Energy*, vol. 41, no. 42, pp. 19218–19230, Nov. 2016, doi: 10.1016/j.ijhydene.2016.07.219.
- [34] Y. Wang, Z. Wang, M. Sun, H. Wang, and Z. Cai, "Effects of fueling distance on combustion stabilization modes in a cavity-based scramjet combustor," *Acta Astronautica*, vol. 155, no. October 2018, pp. 23–32, 2019, doi: 10.1016/j.actaastro.2018.11.005.
- [35] C. Zhang, J. Chang, Y. Zhang, Y. Wang, and W. Bao, "Flow field characteristics analysis and combustion modes classification for a strut/cavity dual-mode combustor," *Acta Astronautica*, vol. 137, pp. 44–51, Aug. 2017, doi: 10.1016/j.actaastro.2017.03.023.
- [36] T. Wang, G. Li, Y. Yang, Z. Wang, Z. Cai, and M. Sun, "Combustion modes periodical transition in a hydrogen-fueled scramjet combustor with rear-wall-expansion cavity flameholder," *International Journal of Hydrogen Energy*, vol. 45, no. 4, pp. 3209–3215, Jan. 2020, doi: 10.1016/j.ijhydene.2019.11.118.
- [37] L. Zhang, J. Liang, M. Sun, and H. Wang, "Experimental investigation of combustion stabilization modes in a cavity-based supersonic combustor with different wall divergence angles," *Proceedings of the Institution of Mechanical Engineers, Part G: Journal of Aerospace Engineering*, vol. 232, no. 10, pp. 1853–1863, 2018, doi: 10.1177/0954410017710270.
- [38] W. Huang, Z. bo Du, L. Yan, and R. Moradi, "Flame propagation and stabilization in dual-mode scramjet combustors: A survey," *Progress in Aerospace Sciences*, vol. 101, no. June, pp. 13–30, 2018, doi: 10.1016/j.paerosci.2018.06.003.

- [39] G. Y. Zhao, M. B. Sun, X. L. Song, X. P. Li, and H. B. Wang, "Experimental investigations of cavity parameters leading to combustion oscillation in a supersonic crossflow," *Acta Astronautica*, vol. 155, no. December 2018, pp. 255–263, 2019, doi: 10.1016/j.actaastro.2018.12.011.
- [40] Q. Yang, J. Chang, W. Bao, and J. Deng, "A mechanism of combustion mode transition for hydrogen fueled scramjet," *International Journal of Hydrogen Energy*, vol. 39, no. 18, pp. 9791–9797, Jun. 2014, doi: 10.1016/j.ijhydene.2014.04.090.
- [41] W. Bao, Q. Yang, J. Chang, Y. Zong, and J. Hu, "Dynamic Characteristics of Combustion Mode Transitions in a Strut-Based Scramjet Combustor Model," *Journal of Propulsion and Power*, vol. 29, no. 5, 2013, doi: 10.2514/1.B34921.
- [42] L. Yan, L. Liao, W. Huang, and L. quan Li, "Nonlinear process in the mode transition in typical strut-based and cavity-strut based scramjet combustors," *Acta Astronautica*, vol. 145, pp. 250–262, Apr. 2018, doi: 10.1016/j.actaastro.2018.01.061.
- [43] J. Chang, L. Wang, W. Bao, Q. Yang, and J. Qin, "Experimental investigation of hysteresis phenomenon for scramjet engine," *AIAA Journal*, vol. 52, no. 2, pp. 447–451, Feb. 2014, doi: 10.2514/1.J052505.
- [44] Z. Yan, Z. Shaohua, C. Bing, and X. Xu, "Hysteresis of mode transition in a dual-struts based scramjet," *Acta Astronautica*, vol. 128, pp. 147–159, Nov. 2016, doi: 10.1016/j.actaastro.2016.07.025.
- [45] X. Zhang, L. Yue, T. Huang, Q. Zhang, and X. Zhang, "Numerical investigation of mode transition and hysteresis in a cavity-based dual-mode scramjet combustor," *Aerospace Science and Technology*, vol. 94, Nov. 2019, doi: 10.1016/j.ast.2019.105420.
- [46] X. Zhang *et al.*, "Experimental study of hysteresis and catastrophe in a cavity-based scramjet combustor," *Chinese Journal of Aeronautics*, Sep. 2021, doi: 10.1016/j.cja.2021.08.008.
- [47] R. S. Pinto, T. Sree Renganathan, S. M. D. Hamid Ansari, and T. M. Muruganandam, "Hysteresis in flame stabilization in a hydrogen fueled supersonic combustor," *International Journal of Hydrogen Energy*, Jun. 2022, doi: 10.1016/j.ijhydene.2022.05.153.
- [48] G. Zhao, J. Du, H. Yang, T. Tang, and M. Sun, "Effects of injection on flame flashback in supersonic crossflow," *Aerospace Science and Technology*, vol. 120, Jan. 2022, doi: 10.1016/j.ast.2021.107226.
- [49] M. B. Sun, X. da Cui, H. B. Wang, and V. Bychkov, "Flame flashback in a supersonic combustor fueled by ethylene with cavity flame holder," *Journal of Propulsion and Power*, vol. 31, no. 3, pp. 976–980, 2015, doi: 10.2514/1.B35580.
- [50] J. Zhang, J. Chang, Z. Wang, L. Gao, and W. Bao, "Flame propagation and flashback characteristics in a kerosene fueled supersonic combustor equipped with strut/wall combined fuel injectors," *Aerospace Science and Technology*, vol. 93, p. 105303, 2019, doi: 10.1016/j.ast.2019.105303.
- [51] S. Zhu, X. Xu, Q. Yang, and Y. Jin, "Intermittent back-flash phenomenon of supersonic combustion in the staged-strut scramjet engine," *Aerospace Science and Technology*, vol. 79, pp. 70–74, 2018, doi: 10.1016/j.ast.2018.05.037.